Polymer Chemistry

ROYAL SOCIETY OF CHEMISTRY

PAPER

View Article Online
View Journal | View Issue

Cite this: *Polym. Chem.*, 2026, **17**, 171

Structure–property relationships in poly(olefin sulfone) copolymers and terpolymers derived from linear and cyclic alkenes

Isaac D. Addo, [a,b] Anna Q. Steele [a,b] and John B. Matson *[a,b]

Poly(olefin sulfone)s (POSs), formed *via* alternating copolymerizations of sulfur dioxide (SO_2) and olefins, remain understudied with respect to systematic structure–property relationships. In this work, we report the synthesis and thermal characterization of five POS copolymers and 24 terpolymers derived from linear alkenes (1-hexene, 1-decene) and cycloalkenes (cyclopentene, cyclohexene, norbornene). All polymers were prepared by free radical polymerization at −30 °C initiated by *tert*-butyl hydroperoxide. Molecular characterization by ^{1}H and ^{13}C NMR spectroscopy, FTIR spectroscopy, and size-exclusion chromatography with multi-angle light scattering (SEC-MALS) confirmed polymer structures and high molecular weights (weight-average molecular weight, M_w = 100–8000 kg mol^{-1}). Thermogravimetric analysis showed decomposition temperatures at 50% weight loss ($T_{d,50\%}$) for the copolymers ranged from 292 to 317 °C, with the highest stability observed in the norbornene-containing copolymers and terpolymers. Differential scanning calorimetry revealed glass transition temperatures (T_g = 46–184 °C) that increased systematically with the incorporation of cyclic comonomers. These results show systematic structure–property relationships in POS *co*- and terpolymers and demonstrate how polymer structure governs thermal behavior, providing guidance for the design of thermally robust sulfone-based polymers for advanced applications.

Received 2nd September 2025,
Accepted 26th November 2025

DOI: 10.1039/d5py00859j

rsc.li/polymers

Introduction

Poly(olefin sulfone)s (POSs) are a unique and historically significant class of polymers. Alternating copolymers formed from olefins and sulfur dioxide (SO_2), POSs have been known for over a century.[1,2] In fact, early studies on POS synthesis contributed heavily to the modern understanding of chain polymerization.[3] Specifically, studies by Snow and Frey[4] as well as Dainton and Ivin[5] in the 1930s and 1940s on copolymerization of SO_2 with olefins brought about the discovery of the ceiling temperature phenomenon and its relationship to critical monomer concentration. Further work in the 1970s by Crawford and Gray established the basic thermal and mechanical properties of a handful of POS copolymers,[6] while Brown and O'Donnell determined kinetic and thermodynamic parameters for the synthesis of poly(1-butene sulfone).[7] Since these early discoveries, POSs have been found to exhibit high transparency, chemical resistance, and good barrier properties.[8–10] However, despite their early promise and contributions to fundamental polymer theory, POSs have gained limited attention in the literature over the past few decades. For example, correlations between molecular structure and thermal properties, especially in terpolymers made from two olefins along with SO_2, are significantly lacking.

Although attention to POSs has been sporadic over the past several decades, they have recently gained renewed interest with both mechanistic studies and applied studies focusing largely on adhesive and lithographic applications.[11,12] For example, in 2010 Lobez and Swager developed POSs as radiation detection materials and as components in degradable composites, demonstrating their potential in stimuli-responsive systems.[13] Sasaki reported on the role of charge-transfer complexes in directing polymer structure and opening pathways to degradable adhesives.[14,15] This work inspired a 2025 report from Hayes and coworkers on reversible polyurethane adhesives containing sulfone units.[16] Similarly, Moore and coworkers described in 2016 the base-triggered degradation of vinyl ester–sulfone copolymers, showing tunable depolymerizability and controlled breakdown.[17] In another area, a pair of 2017 papers by Jia and coworkers focused on the degradation mechanism and optical properties of poly(norbornene sulfone)s.[18,19] Finally, one particularly promising application of POSs is in photoresist technology, where their ability to

[a]*Department of Chemistry, Virginia Tech, Blacksburg, Virginia 24061, USA. E-mail: jbmatson@vt.edu*
[b]*Macromolecules Innovation Institute, Virginia Tech, Blacksburg, Virginia 24061, USA*

depolymerize under mild conditions enables their use as positive tone resists. Their usefulness in lithography dates back to the early 1970s, when they were identified and evaluated in electron-beam lithography because of their susceptibility to chain scission and subsequent depolymerization upon exposure to high-energy radiation.[20,21] This led to the brief commercialization of poly(1-butene sulfone) as a positive-tone photoresist in electron-beam lithography.[22–24] However, their broader usage has been limited partly due to a lack of data on their structure–property relationships. Beyond POSs, aromatic polysulfones represent a major class of engineering polymers,[25] and other types of aliphatic polysulfones have been recently reported such as periodic copolymers[26] and homopolymers with applications including optoelectronic materials,[27] mechanophores that release SO_2,[28] and polymers for therapeutic delivery of SO_2.[29] The field of aliphatic SO_2-containing polymers is growing in importance, creating a demand for fundamental structure–property studies.

Here we set out to investigate a series of POS copolymers and terpolymers (Fig. 1) designed with a range of monomer types and polymer compositions. We envision that developing structure–property relationships of POSs, specifically focusing here on thermal properties, will provide key fundamental understandings to guide the further development of POSs as functional materials. Despite reports of thermal degradation data for a few linear and cyclic POSs, there has been no systematic effort to correlate structural features such as linear *versus* cyclic olefin monomers, length of alkyl substitution in linear olefin monomers, or linear-to-cycloalkene ratio with properties like decomposition temperature (T_d) and glass transition temperature (T_g). We hypothesized that these structural differences would significantly influence the thermal stability and transitions of POSs, particularly given their highly alternating backbones and the steric effects imposed by the bulky sulfone group. Through this work, we sought to establish structure–property relationships that would provide a foundation for the rational design of POSs in future material applications.

Results and discussion

Synthesis of copolymers and terpolymers

We selected two linear alkenes (1-hexene and 1-decene) and three cycloalkenes (cyclopentene, cyclohexene, and norbornene) for this study. These monomer selections were guided by the need for electron rich olefins, which play a crucial role in the propagation mechanism of POS copolymerization. This alternating nature associated with POSs requires that olefin comonomers must not only be electron-rich, but also fairly sterically unhindered and at least moderately soluble in SO_2 to support efficient enchainment throughout the chain polymerization process.[30] Additionally, these abundant and low-cost monomers were chosen to provide diverse structural features: 1-hexene and 1-decene are 1-alkenes with linear alkyl chains of varying lengths, while cyclopentene and cyclohexene introduce cyclic structures into the POS backbone with varying ring sizes. Norbornene, which has a rigid, bicyclic structure, was selected as the third cycloalkene to assess how a backbone bicyclic norbornane unit would affect thermal properties. These monomers are liquids at room temperature, with the exception of norbornene, which is a solid. The chemical structures of these five monomers are shown in Fig. 2A.

POSs are typically synthesized *via* free radical copolymerization (FRP), where an olefin monomer, either linear or cyclic, reacts with SO_2 in the presence of a radical initiator, most commonly *tert*-butyl hydroperoxide (*t*BuOOH) due to its ability to generate a high concentration of initiating radicals even at low temperatures.[31,32] Reaction temperatures in the range of −80 to −20 °C are common in order to maintain SO_2 below its boiling point of −10 °C and to avoid exceeding the low ceiling temperature of some POSs. All reactions are typically performed under an inert nitrogen atmosphere.[33] The reaction proceeds through a 1 : 1 alternating copolymerization mechanism due to the strong electron-withdrawing nature of SO_2, which has been suggested to form a charge-transfer complex with the olefin, stabilizing the propagating radical and directing alternation.[34] As a result, the POS backbone structure contains alternating sulfone (–SO_2–) groups with two-carbon units derived from the olefin monomer.[35] POS synthesis *via*

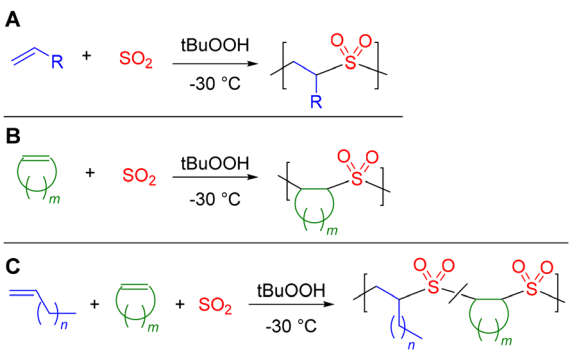

Fig. 1 Generalized synthetic routes to POS copolymers and terpolymers, including linear POS copolymers (A); cyclic POS copolymers (B); and POS terpolymers (C). All routes involve free radical polymerization initiated by *t*BuOOH.

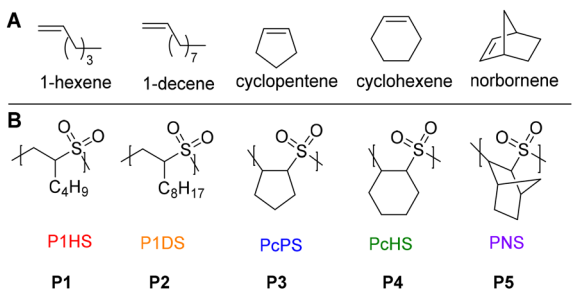

Fig. 2 (A) Chemical structures of monomers. (B) POS copolymers including poly(1-hexene sulfone) (P1HS, **P1**), poly(1-decene sulfone) (P1DS, **P2**), poly(cyclopentene sulfone) (PcPS, **P3**), poly(cyclohexene sulfone) (PcHS, **P4**), and poly(norbornene sulfone) (PNS, **P5**).

FRP generally forms high molecular weight polymers with good yields.

We commenced our study by synthesizing a series of five POS copolymers (Fig. 2B), each obtained from FRP of SO_2 with the olefin monomer at −30 °C and initiated by *t*BuOOH. Each resulting copolymer was named according to its olefin monomer precursor; for example, the copolymer derived from 1-hexene with SO_2 was denoted P1HS for poly(1-hexenesulfone). Liquid SO_2, which functions as both a monomer and solvent, was condensed directly into the reaction vessel, and polymerizations were caried out in bulk, with the exception of norbornene, which required toluene or dichloromethane to aid in dissolution. All polymerizations were complete within 30 min, as determined through ^{1}H NMR analysis of aliquots to observe monomer conversion. Poly(norbornene sulfone) (PNS, **P5)** formed faster than all others and was completed within 10 min. The resulting polymers were all isolated by precipitation and filtration as white solids in good yields. Attempts to copolymerize *cis*-cyclooctene with SO_2 at −30 °C were unsuccessful, presumably due to the low ceiling temperature of the resulting copolymer. The results of the copolymerizations are summarized in Table 1.

^{1}H and ^{13}C NMR spectra of the obtained copolymers confirmed the expected POS structures (Fig. S10–S14). All copolymers were obtained in good isolated yields, indicating efficient monomer incorporation and minimal side reactions. Corroborating the ^{1}H and ^{13}C NMR spectra, FTIR spectroscopy confirmed the incorporation of the sulfone moiety into the polymer backbone for all five POS copolymers (Fig. 3A and Fig. S3–S9). Two strong, characteristic absorption bands at ~1100–1120 cm^{-1} for symmetric S=O stretching and ~1280–1300 cm^{-1} for asymmetric S=O stretching appeared in all five spectra. Additionally, the spectra for the copolymers showed the absence of the characteristic C=C band at ~1620–1680 cm^{-1}. These results confirm the successful olefin and SO_2 incorporation into the copolymer backbones.

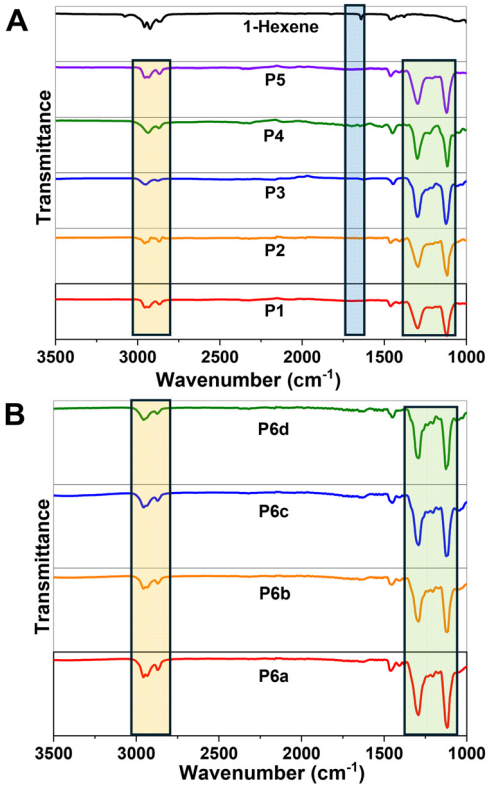

Fig. 3 (A) Normalized FTIR spectra of the copolymers, **P1–P5,** highlighting C–H stretches shaded in light orange (~2950 cm^{-1}) and SO_2 stretches shaded in light green (~1290 and ~1120 cm^{-1}) compared with 1-hexene monomer with the C=C stretch shaded in light blue. (B) FTIR spectra of the terpolymers **P6a–d** (HS : cPS) highlighting the C–H stretches shaded in light orange (~2950 cm^{-1}) and SO_2 stretches shaded in light green (~1290 and ~1120 cm^{-1}).

Table 1 Molecular weight characterization of POS copolymers

Copolymer number	Copolymer name	Yield (%)	d*n*/d*c*[a]	$M_{w,SEC}$[b] (kg mol^{-1})
P1	P1HS	83	0.095	970
P2	P1DS	86	0.075	1820
P3	PcPS	84	—	—
P4	PcHS	77	0.092	100
P5	PNS	90	0.051	6510

[a] For all copolymers, d*n*/d*c* values were determined using the 100% mass recovery method after verifying good accuracy of the method through an offline d*n*/d*c* measurement for P1HS (**P1**) (Fig. S72). Reported values represent the average of three replicate runs (Table S1). PcPS (**P3**) was not sufficiently soluble in the mobile phase for SEC analysis. [b] $M_{w,SEC}$ values were determined in THF eluent (mobile phase) at 30 °C on two PLGel mixed-B columns with Wyatt differential refractive index (dRI) and multi-angle light scattering (MALS) detectors. Because the chromatographic separation was poor in THF, only the M_w value is reported because the M_n value is unreliable.

Size exclusion chromatography with multi-angle light scattering (SEC-MALS) in tetrahydrofuran (THF) was used to characterize each copolymer. The SEC-MALS results (Table 1) showed that M_w values ranged from 100–6510 kg mol^{-1} and showed that **P5** gave the highest M_w among the copolymers studied, which is consistent with the high reactivity of norbornene in radical copolymerizations with SO_2.[36,37] All copolymers were soluble in THF at room temperature, with the exception of **P3**, which exhibited limited solubility even with extended sonication. Asymmetric SEC-MALS traces revealed that all five POS copolymers exhibited some "dragging" on the columns. This effect led to peak broadening, a phenomenon that affects the accuracy of M_n and $Đ$ values.[38] As a result, only the M_w values are reliable here. We also performed SEC-MALS using other mobile phases (DMAc, DMF), but we also observed "dragging" on the columns in these solvents as well.

Next, we set out to synthesize the targeted POS terpolymers. We chose a structural library of terpolymers using combinations of linear 1-alkenes and cyclic olefins. The library included 24 terpolymers, synthesized using each combination of the 5 possible linear 1-alkene and cyclic olefin formulations with four different feed ratios for each (molar ratios of 80 : 20,

60 : 40, 40 : 60, and 20 : 80), providing a systematic study of structural effects on polymer properties (Fig. 4).

The same polymerization conditions used for copolymer synthesis were maintained for terpolymer synthesis. For POS terpolymers, monomer feed ratios were used as noted in Table 2, and polymerizations were carried out to near-complete conversion. Given the challenges associated with accurately determining the reactivity ratios in ternary systems,[39] we did not attempt to measure reactivity ratios in this work. For terpolymers containing norbornene, the monomer was first dissolved in toluene prior to transfer into the reaction flask, as was done for the norbornene copolymers. The resulting terpolymers were isolated by precipitation in good yields.

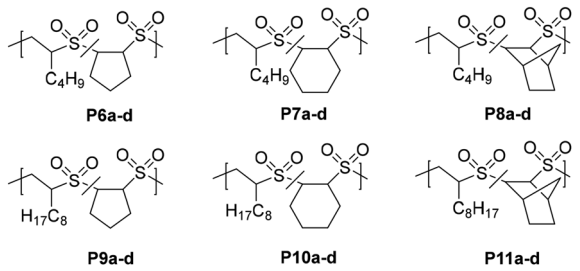

Fig. 4 POS terpolymers of various formulations in ratios of 80 : 20, 60 : 40, 40 : 60, and 20 : 80.

The compositions of the resulting terpolymers were determined by ^{1}H NMR spectroscopy. Fig. 5 shows example ^{1}H NMR spectra of copolymers P1HS (**P1**, bottom), PcPS (**P3**, middle), and the one of the terpolymers P1HS-*co*-PcPS (**P6a**, top). The spectrum of **P1** showed characteristic signals at $\delta \approx 3.8$ ppm (b) and $\delta \approx 3.3$ ppm (a), corresponding to the methylene and methine protons adjacent to the sulfone group. The backbone cyclopentyl unit in **P3** displayed a distinct multiplet at $\delta \approx 4.2$ ppm (c), corresponding to methine protons adjacent to the sulfone groups. The terpolymer **P6a** showed signals from both homopolymers, including peaks at $\delta \approx 4.2$ ppm (c, from **P3**) and $\delta \approx 3.8$ and 3.3 ppm (b and a, from **P1**), confirming successful incorporation of both monomer units. The relative integration of the diagnostic peaks in the **P6a** spectrum (Fig. S15) was determined to be 81 : 19 (**P1** : **P3**), which closely matches the targeted 80 : 20 molar feed ratio, showing successful copolymerization. Similarly, the ^{1}H NMR spectra of additional terpolymers showed peak patterns consistent with their target compositions, with the exception of norbornene-containing terpolymers where peak overlap prevented accurate composition analysis (Fig. S15–S50). As in the copolymers, FTIR spectroscopy confirmed the incorporation of sulfone group into the polymer backbone for all 24 terpolymers (Fig. 3B and Fig. S4–S9).

SEC-MALS was used to determine the M_w values of the terpolymers. Similar to the copolymers, chromatography quality was variable but generally suggested interactions of the terpo-

Table 2 Synthesis and characterization of POS terpolymers

Polymer number	Terpolymer structure	Target feed[a]	Composition[b]	Yield (%)	dn/dc [c]	$M_{w,SEC}$ [d] (kg mol^{-1})
P6a	P1HS-*co*-PcPS	80 : 20	81 : 19	84	0.094	990
P6b	P1HS-*co*-PcPS	60 : 40	64 : 36	88	0.094	1440
P6c	P1HS-*co*-PcPS	40 : 60	47 : 53	79	0.093	1830
P6d	P1HS-*co*-PcPS	20 : 80	28 : 72	80	0.093	2550
P7a	P1HS-*co*-PcHS	80 : 20	72 : 28	78	0.094	210
P7b	P1HS-*co*-PcHS	60 : 40	54 : 46	74	0.094	140
P7c	P1HS-*co*-PcHS	40 : 60	32 : 68	79	0.093	220
P7d	P1HS-*co*-PcHS	20 : 80	17 : 83	72	0.093	300
P8a	P1HS-*co*-PNS	80 : 20	80 : 20[e]	89	0.086	1280
P8b	P1HS-*co*-PNS	60 : 40	60 : 40[e]	89	0.077	1800
P8c	P1HS-*co*-PNS	40 : 60	40 : 60[e]	86	0.069	2940
P8d	P1HS-*co*-PNS	20 : 80	20 : 80[e]	79	0.060	1610
P9a	P1DS-*co*-PcPS	80 : 20	77 : 23	93	0.079	780
P9b	P1DS-*co*-PcPS	60 : 40	64 : 36	81	0.081	1370
P9c	P1DS-*co*-PcPS	40 : 60	43 : 57	89	0.085	920
P9d	P1DS-*co*-PcPS	20 : 80	23 : 77	90	0.088	1470
P10a	P1DS-*co*-PcHS	80 : 20	73 : 27	85	0.080	1630
P10b	P1DS-*co*-PcHS	60 : 40	53 : 47	78	0.083	1485
P10c	P1DS-*co*-PcHS	40 : 60	33 : 67	75	0.086	1010
P10d	P1DS-*co*-PcHS	20 : 80	19 : 81	71	0.089	1070
P11a	P1DS-*co*-PNS	80 : 20	80 : 20[e]	85	0.070	630
P11b	P1DS-*co*-PNS	60 : 40	60 : 40[e]	80	0.065	660
P11c	P1DS-*co*-PNS	40 : 60	40 : 60[e]	89	0.061	950
P11d	P1DS-*co*-PNS	20 : 80	20 : 80[e]	92	0.056	8240

[a] Target feed indicates the molar feed ratio of linear alkene to cycloalkene in the reaction mixture. [b] Polymer composition was determined by analysis of the terpolymer ^{1}H NMR spectra. [c] All terpolymer dn/dc values were determined by using measured dn/dc values of the copolymers (Table S1) and their relative weight fractions using the formula described previously.[38] Limited solubility prevented measurement of the dn/dc value of PcPS (**P3**), so it was assumed to have the same dn/dc value as PcHS (**P4**) due to their structural similarity, and this value was used in calculating the $M_{w,SEC}$ values of the corresponding terpolymers. [d] $M_{w,SEC}$ values were determined in THF eluent at 30 °C on two PLGel mixed-B columns with Wyatt differential refractive index (dRI) and multi-angle light scattering (MALS) detectors. [e] Polymer composition for **P8a–d** and **P11a–d** were assumed to match the target feed ratios because overlapping peaks in the ^{1}H NMR spectra prevented accurate integration. This assumption allowed dn/dc values to be calculated.

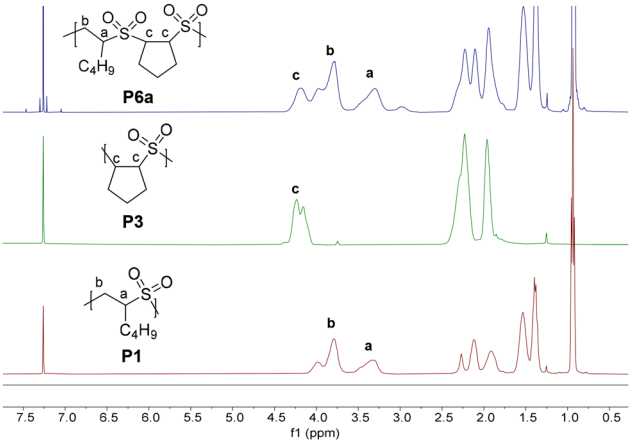

Fig. 5 ^{1}H NMR spectra comparing **P1HS-*co*-PcPS** (**80** : **20**) with copolymers **P1** (**P1HS**) and **P3** (**PcPS**) in $CDCl_3$. Diagnostic protons are labeled as 'a', 'b', and 'c'.

lymers with the stationary phase and aggregation in some cases. Table 2 compiles the results of the different formulations with their $M_{w,SEC}$ values. The terpolymers ranged from approximately 140–8240 kg mol^{-1}, depending on the backbone structure and feed composition. These results confirmed the successful synthesis of high molecular weight and compositionally diverse POS terpolymers ready for thermal studies.

Thermal stability of copolymers and terpolymers

The thermal stability of POS copolymers **P1–P5** was systematically investigated using thermogravimetric analysis (TGA). The TGA thermograms (Fig. 6A) showed the percentage weight loss as a function of temperature, providing insight into the decomposition behavior of the copolymers. However, it is important to note that the initial weight loss observed as "dips" in the TGA curves in the range of 100–200 °C. These features persisted despite drying all samples in a vacuum oven at 70 °C, an extended equilibration period, and an early heating cycle to remove any remaining volatiles. To assess whether this behavior was due to sample microstructure or batch variation, each copolymer was resynthesized, and the same behavior was observed in all runs. We conclude that these early weight losses are inherent to the copolymers and may represent the onset of chemical decomposition rather than residual impurities. However, these early weight losses were typically only 5–10% of the total sample mass.

Based on the TGA thermograms of the five copolymers, we determined that $T_{d,50\%}$ values represent the most reliable relative indicator of thermal stability. The $T_{d,50\%}$ values for the five copolymers showed a thermal stability trend as **P5** > **P4** > **P3** > **P2** > **P1**, although not all differences are likely significant (Table 3). This trend showed the influence of monomer structure on decomposition resistance. **P5**, which incorporates a rigid norbornene unit, exhibited the highest $T_{d,50\%}$ due to restricted backbone mobility and enhanced chain rigidity. **P3** and **P4**, containing cyclic repeat units, also showed elevated

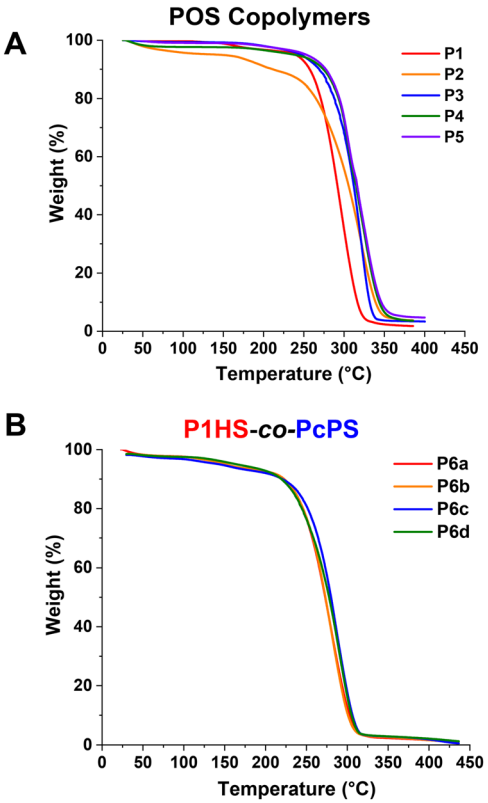

Fig. 6 (A) TGA thermograms of POS copolymers **P1–P5**. (B) TGA thermograms of **P1HS-*co*-PcPS** (**P6a–d**).

Table 3 Thermal characterization of POS copolymers

Polymer number	$T_{d,5\%}$ [a] (°C)	$T_{d,10\%}$ [a] (°C)	$T_{d,50\%}$ [a] (°C)	T_g [b] (°C)
P1	240	257	292	74
P2	145	211	306	49
P3	247	269	312	184
P4	238	274	315	175
P5	238	273	317	179

[a] T_d values were measured at a ramp rate of 20 °C min^{-1} under nitrogen. The temperatures at which the weight loss of the samples reached 5% ($T_{d,5\%}$), 10% ($T_{d,10\%}$), and 50% ($T_{d,50\%}$) are listed. [b] T_g values were determined by DSC with a 10 °C min^{-1} heating and cooling ramp; data reported are from the second heat cycle.

thermal stability with $T_{d,50\%}$ values above 300 °C. In contrast, **P1** and **P2**, which both contained flexible, linear alkyl side chains, exhibited the lowest $T_{d,50\%}$ values. Historically, POSs have been reported to suffer from poor thermal stability, which has hindered their broader commercialization. In many cases, the decomposition temperature falls below the polymer's softening point, limiting processability.[40] However, in this study, all copolymers showed $T_{d,50\%}$ values exceeding 200 °C, indicating sufficient thermal stability for processing in various applications, including photoresist technologies. Although the specific degradation pathway was not the focus of this study, the persistent dips observed in the TGA thermograms suggest a multi-step degradation mechanism. It is

speculated that the decomposition involves homolytic cleavage of the sulfone group, mainly leading to the evolution of SO_2 and olefins, common degradation products of POS systems.[41]

The thermal stability of POS terpolymers was evaluated by TGA (Table 4). Many of these samples also showed small initial mass losses in the TGA curves. The terpolymers were resynthesized to verify reproducibility, and the same behavior was consistently observed. $T_{d,50\%}$ values across the terpolymer series ranged from 216 °C to 305 °C. However, within individual terpolymer series, no consistent or systematic trend in $T_{d,50\%}$ was observed as a function of monomer composition. For example, in the **P6** series, $T_{d,50\%}$ varied from 273 °C to 281 °C across the four formulations (Fig. 6B), while the four samples in the **P9** series ranged from 282 °C to 305 °C with no clear ordering by feed ratio. This lack of compositional dependence likely shows the structural complexity inherent in these terpolymers. Despite controlled monomer feeds, differences in reactivity ratios can lead to a range of polymer compositions in each sample, resulting in chains with highly variable sequence distributions. Additionally, differences in the electronic and steric properties of the comonomer substituents can result in irregular packing, eliminating any simple correlation between feed ratio and thermal stability. $T_{d,50\%}$ data suggest that adjusting comonomer feed ratio alone is insufficient to precisely control the thermal stability of POS copolymers. We speculate that achieving predictable thermal performance will require precise control over sequence distribution to sufficiently link structure with thermal properties. Future work will be directed toward detailed analysis of sequence distributions and exploration of polymerization kinetics to better correlate structure with thermal decomposition properties. Despite the lack of a clear trend, all terpolymers exhibited high thermal stability with $T_{d,50\%}$ > 200 °C, making them suitable for a range of applications that require resistance to harsh thermal environments.

Next, T_g values of the copolymers **P1–P5** were measured using differential scanning calorimetry (DSC). Results are summarized in Table 3 and Fig. 7A. The lowest T_g was observed in **P2** (49 °C), which incorporates a flexible, linear 1-decene comonomer. The long alkyl chain introduces free volume and promotes chain mobility, leading to a low glass transition. **P1**, also based on a linear olefin (1-hexene), showed a modest T_g increase (74 °C), consistent with a shorter side chain. In contrast, the highest T_g values were observed in copolymers with cyclic and bicyclic comonomers: **P3** exhibited the highest T_g (184 °C), followed closely by **P5** (179 °C) and **P4** (175 °C). These elevated T_g values are due to the restricted rotational freedom and increased chain stiffness imparted by cyclic structures. This trend highlights the importance of monomer structure in tuning thermal performance. Incorporating cyclic olefins into POS copolymers offers a pathway to enhance their thermal stability and improve application range in high temperature environments such as photolithography. DSC traces did not show any melting temperature (T_m), suggesting the expected amorphous character of these materials.

The T_g values of the POS terpolymer series (Table 4) showed clear and systematic trends as a function of comono-

Table 4 Thermal characterization of POS terpolymers

Polymer number	$T_{d,5\%}$ [a] (°C)	$T_{d,10\%}$ [a] (°C)	$T_{d,50\%}$ [a] (°C)	T_g [b] (°C)
P6-a	152	222	273	82
P6-b	180	228	274	93
P6-c	176	231	281	117
P6-d	192	225	279	145
P7-a	146	209	264	73
P7-b	151	207	264	86
P7-c	161	216	269	92
P7-d	152	203	262	115
P8-a	158	225	275	76
P8-b	180	235	283	79
P8-c	187	230	288	83
P8-d	221	252	294	90
P9-a	206	226	282	51
P9-b	192	224	289	60
P9-c	202	238	293	138
P9-d	188	237	305	155
P10-a	142	155	216	50
P10-b	148	162	229	58
P10-c	130	140	238	76
P10-d	132	143	243	95
P11-a	165	189	276	46
P11-b	137	155	297	52
P11-c	136	160	277	88
P11-d	221	256	305	103

[a] T_d values were measured at a ramp rate of 20 °C min^{-1} under nitrogen. The temperatures at which the weight loss of the samples reached 5% ($T_{d,5\%}$), 10% ($T_{d,10\%}$), and 50% ($T_{d,50\%}$) are listed. [b] T_g values were determined by DSC with a 10 °C min^{-1} heating and cooling ramp; data reported are from the second heat cycle.

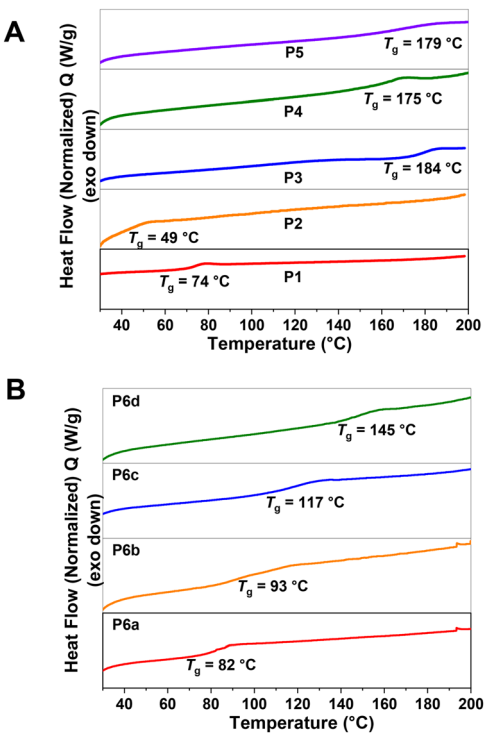

Fig. 7 (A) DSC traces for POS copolymers **P1–P5**. (B) DSC traces for **P6a–d**.

mer feed ratio. In all six series, T_g values increased systematically with increasing content of rigid cycloalkene comonomer in the feed. For example, in the **P6** series (Fig. 7b), T_g increased from 82 °C for **P6a** to 145 °C for **P6d**. Similar upward trends were seen in **P7** (73–115 °C), **P8** (76–90 °C), **P9** (51–155 °C), **P10** (50–95 °C), and **P11** (46–103 °C) (Fig. S66–71). These systematic increases in T_g showed the influence of comonomer composition on chain mobility. Incorporation of stiffer or more sterically hindered cycloalkenes restricted segmental motion along the polymer backbone, raising T_g. In these POS terpolymer systems, comonomers with bulkier substituents around the sulfone linkage likely impede rotational freedom. As their proportion increased, the T_g increased. Unlike thermal decomposition temperatures, which showed no consistent trend with feed ratio, T_g was strongly influenced by the average segmental composition rather than the precise sequence distribution. Overall, these results demonstrate that while controlling thermal decomposition in POS systems is challenging due to structural complexity, T_g can be systematically and predictably tuned *via* comonomer feed composition.

Conclusions

In this work, we synthesized and characterized a series of POS copolymers and terpolymers derived from both linear and cyclic alkenes to systematically evaluate the influence of monomer structure on thermal properties. Using a diverse set of monomers including flexible linear 1-alkenes and more rigid cycloalkenes, we studied how variations in chain flexibility and rigidity, as well as steric bulk, affected polymer thermal behavior. All POS copolymers and terpolymers were successfully synthesized *via* FRP yielding high molecular weight materials with good incorporation efficiency confirmed by NMR and FTIR spectroscopy. SEC-MALS analysis confirmed high molecular weights for each copolymer and terpolymer, and thermal analysis revealed key structure–property relationships. $T_{d,50\%}$ values exceeded 200 °C for nearly all samples, and T_g values depended strongly on alkene structure for the copolymers, with copolymers containing cycloalkenes exhibiting T_g values exceeding 170 °C. Terpolymers containing higher proportions of cycloalkene comonomers showed increased T_g values. These results highlight the importance of polymer design in tuning segmental mobility and thermal transitions in POSs. The ability to tailor T_g through feed composition, even in complex terpolymer systems, presents a valuable pathway for advanced materials and provides a foundation for the rational design of thermally robust POS materials for use in emerging technologies such as lithography, adhesives, and semiconductor packaging.

Conflicts of interest

There are no conflicts to declare.

Data availability

The data that support the findings of this study are openly available in figshare.com at https://doi.org/10.6084/m9.figshare.30005146, reference number 30005146.

Supplementary information including safety and hazards statement, materials and methods, complete set of FTIR and NMR spectra, SEC traces, TGA thermograms, DSC curves, and d*n*/d*c* determination experiments is available. See DOI: https://doi.org/10.1039/d5py00859j.

Acknowledgements

This work was supported by the Semiconductor Research Corporation (SRC, 2024-ES-3231) and the National Science Foundation (NSF, CHE-2003662). The authors gratefully acknowledge Dr. Ryan J. Carrazzone and Bob Leet (Intel Corporation) for their valuable suggestions. We also thank Brian Puckett (Micron) as well as Cory Fronk and Tim Yeakley (Texas Instruments), for their insightful input. This work made use of shared facilities in the Material Characterization Lab (MCL) which is funded and managed by Virginia Tech. We also thank Mark McCrary and Dr. Erin C. Jackson in the lab of Prof. Robert Moore for assistance with thermal analysis. We also thank Prof. Chris Bates and Dr. Amanda Strom (University of California, Santa Barbara) for helpful analyses and suggestions.

References

1 W. Solonina, *Russ. J. Phys. Chem. A*, 1898, **30**, 826–842.
2 *Chem. Zentralbl.*, 1899, **70**, 248–249.
3 C. M. Fellows, R. G. Jones, D. J. Keddie, C. K. Luscombe, J. B. Matson, K. Matyjaszewski, J. Merna, G. Moad, T. Nakano and S. Penczek, Terminology for chain polymerization (IUPAC Recommendations 2021), *Pure Appl. Chem.*, 2022, **94**(9), 1093–1147.
4 R. D. Snow and F. E. Frey, The reaction of sulfur dioxide with olefins: the ceiling temperature phenomenon, *J. Am. Chem. Soc.*, 1943, **65**(12), 2417–2418.
5 F. S. Dainton and K. J. Ivin, Reversibility of the Propagation Reaction in Polymerization Processes and its Manifestation in the Phenomenon of a 'Ceiling Temperature', *Nature*, 1948, **162**(4122), 705–707.
6 J. E. Crawford and D. N. Gray, Preparation and properties of some poly(alpha–olefin sulfones), *J. Appl. Polym. Sci.*, 1971, **15**(8), 1881–1888.
7 J. Brown and J. O'Donnell, Gas–phase copolymerization of sulfur dioxide and butene–1, *J. Polym. Sci., Part A-1*, 1972, **10**(7), 1997–2004.
8 T. Kitamura, N. Tanaka, A. Mihashi and A. Matsumoto, Soluble and thermally stable polysulfones prepared by the regiospecific and alternating radical copolymerization of 2,

4-hexadiene with sulfur dioxide, *Macromolecules*, 2010, **43**(4), 1800–1806.
9 T. N. Bowmer and J. H. O'Donnell, Radiation Degradation of Poly(olefin Sulfone)s: A Volatile Product Study, *J. Macromol. Sci., Part A:Pure Appl. Chem.*, 1982, **17**(2), 243–263.
10 R. Okutsu, Y. Suzuki, S. Ando and M. Ueda, Poly(thioether sulfone) with high refractive index and high Abbe's number, *Macromolecules*, 2008, **41**(16), 6165–6168.
11 X.-F. Zhu, X.-Y. Lu, H. Qi, Y. Wang and G.-P. Wu, Sulfur-containing polymers derived from SO_2: synthesis, properties, and applications, *Polym. Chem.*, 2022, **13**(37), 5282–5299.
12 T. Sasaki, K. Van Le and Y. Naka, Poly(olefin sulfone)s, *Alkenes*, 2018, 121–144.
13 J. M. Lobez and T. M. Swager, Disassembly of elastomers: poly (olefin sulfone)– silicones with switchable mechanical properties, *Macromolecules*, 2010, **43**(24), 10422–10426.
14 H. Yaguchi and T. Sasaki, Photoinduced depolymerization of poly(olefin sulfone)s possessing photobase generating groups in the side chain, *Macromolecules*, 2007, **40**(26), 9332–9338.
15 T. Sasaki, S. Hashimoto, N. Nogami, Y. Sugiyama, M. Mori, Y. Naka and K. Van Le, Dismantlable thermosetting adhesives composed of a cross-linkable poly(olefin sulfone) with a photobase generator, *ACS Appl. Mater. Interfaces*, 2016, **8**(8), 5580–5585.
16 M. J. Hyder, J. Godleman, A. M. Chippindale, J. E. Hallett, T. Zinn, J. L. Harries and W. Hayes, Thermally and base-triggered "Debond-on-Demand" chain-extended polyurethane adhesives, *Macromolecules*, 2025, **58**(1), 681–696.
17 C. M. Possanza Casey and J. S. Moore, Base-Triggered Degradation of Poly(vinyl ester sulfone)s with Tunable Sensitivity, *ACS Macro Lett.*, 2016, **5**(11), 1257–1260.
18 X. Liu, Y. Zhi, S. Shan, H. Su and Q. Jia, Tunable thermal degradation and refractive index of poly(norbornene sulfone)s via two different polymerization methods, *J. Appl. Polym. Sci.*, 2017, **134**(9), 44534.
19 X. Liu, X. Guo, Y. Zhi, S. Shan, Y. Ni and Q. Jia, Kinetics and mechanism of the thermal degradation for the synthesis of poly(norbornene sulfone)s by two different polymerization methods, *Polym. Adv. Technol.*, 2017, **28**(11), 1438–1447.
20 J. Brown and J. O'Donnell, The degradation of poly(butene-1 sulfone) during γ irradiation, *Macromolecules*, 1970, **3**(2), 265–267.
21 J. Brown and J. O'Donnell, γ Radiolysis of poly(butene-1 sulfone) and poly (hexane-1 sulfone), *Macromolecules*, 1972, **5**(2), 109–114.
22 M. J. Bowden and L. F. Thompson, Electron irradiation of poly(olefin sulfones). Application to electron beam resists, *J. Appl. Polym. Sci.*, 1973, **17**(10), 3211–3221.
23 M. J. Bowden, Electron irradiation of polymers and its application to resists for electron-beam lithography, *Crit. Rev. Solid State Mater. Sci.*, 1979, **8**(3), 223–264.
24 M. Bowden and L. Thompson, Poly(butene-1 sulfone) as a Positive Electron Resist, in, *Appl. Polym. Symp*, 1974, **23**, 99.
25 C. Dizman, M. A. Tasdelen and Y. Yagci, Recent advances in the preparation of functionalized polysulfones, *Polym. Int.*, 2013, **62**(7), 991–1007.
26 K. Gao, X. Wang, T. Wang, S. Song and C. Zhu, Preparation of Degradable and Sequence–Controlled Aliphatic Polysulfones by Group Transfer Radical Polymerization, *Angew. Chem., Int. Ed.*, 2025, **64**(16), e202500153.
27 A. Matsumoto, S. Lee and H. Okamura, Molecular design of diene monomers containing an ester functional group for the synthesis of poly(diene sulfone)s by radical alternating copolymerization with sulfur dioxide, *J. Polym. Sci., Part A:Polym. Chem.*, 2015, **53**(8), 1000–1009.
28 Y. Sun, W. J. Neary, X. Huang, T. B. Kouznetsova, T. Ouchi, I. Kevlishvili, K. Wang, Y. Chen, H. J. Kulik and S. L. Craig, A thermally stable SO_2-releasing mechanophore: facile activation, single-event spectroscopy, and molecular dynamic simulations, *J. Am. Chem. Soc.*, 2024, **146**(15), 10943–10952.
29 A. Mondal, S. Paul and P. De, Sulfur dioxide (SO_2) releasing polymeric systems: Design, synthesis, and potential biomedical applications, *ACS Appl. Polym. Mater.*, 2024, **6**(15), 8950–8965.
30 N. Yao and Z. L. Wang, *Handbook of microscopy for nanotechnology*, Springer, 2005.
31 M. Matsuda and H. H. Thoi, Propagation Mechanism of Radical Copolymerization of Sulfur Dioxide and Vinyl Chloride., *J. Macromol. Sci., Chem.*, 1977, **11**(8), 1423–1437.
32 O. Ito and M. Matsuda, A new dual–parameter for reactivities of vinyl monomers toward free–radicals, *J. Polym. Sci., Part A:Polym. Chem.*, 1990, **28**(7), 1947–1963.
33 T. Sasaki, K. Van Le and Y. Naka, Poly(olefin sulfone)s, *Alkenes*, 2018, 147–161.
34 S. A. Chambers, A. H. Fawcett, S. Fee, J. F. Malone and U. Smyth, Microstructure of poly(but-2-ene sulfone) and the role of the SO_2-olefin charge-transfer complex in the polymerization reaction, *Macromolecules*, 1990, **23**(10), 2757–2765.
35 R. Cais, J. O'Donnell and F. Bovey, Copolymerization of styrene with sulfur dioxide. Determination of the monomer sequence distribution by carbon-13 NMR, *Macromolecules*, 1977, **10**(2), 254–260.
36 N. Zutty, C. Wilson III, G. Potter, D. Priest and C. Whitworth, Copolymerization studies. VI. Spontaneous copolymerization of bicyclo[2.2. 1]hept–2–ene and sulfur dioxide. Evidence for propagation by biradical coupling, *J. Polym. Sci., Part A: Gen. Pap.*, 1965, **3**(8), 2781–2799.
37 E. H. Hill and J. R. Caldwell, Polysulfones of norbornene and derivatives, *J. Polym. Sci., Part A: Gen. Pap.*, 1964, **2**(3), 1251–1255.
38 J. B. Matson, A. Q. Steele, J. D. Mase and M. D. Schulz, Polymer characterization by size-exclusion chromatography with multi-angle light scattering (SEC-MALS): a tutorial review, *Polym. Chem.*, 2024, **15**(3), 127–142.

39 J. Hazell and K. Ivin, Relative reactivities of olefines in polysulphone formation, *Trans. Faraday Soc.*, 1962, **58**, 176–185.
40 M. J. Bowden, L. F. Thompson, W. Robinson and M. Biolsi, Thermal degradation of poly(1-butene sulfone), *Macromolecules*, 1982, **15**(5), 1417–1422.
41 F. S. Dainton and K. J. Ivin, The kinetics of polysulphone formation II. The formation of 1-butene polysulphone in the region of the ceiling temperature, *Proc. R. Soc. London, Ser. A*, 1952, **212**(1109), 207–220.